Nanoscale

COMMUNICATION

View Article Online
View Journal | View Issue

Cite this: Nanoscale, 2016, 8, 5820

Received 7th December 2015,
Accepted 16th February 2016

DOI: 10.1039/c5nr08692b

www.rsc.org/nanoscale

Enhancing light emission efficiency without color change in post-transition metal chalcogenides†

Cong Wang,‡[a,b] Shengxue Yang,‡[c] Hui Cai,‡[d] Can Ataca,*[e] Hui Chen,[f] Xinzheng Zhang,[a] Jingjun Xu,[a] Bin Chen,[d] Kedi Wu,[d] Haoran Zhang,[b] Luqi Liu,[b] Jingbo Li,*[f] Jeffrey C. Grossman,[e] Sefaattin Tongay*[d] and Qian Liu*[a,b]

Two-dimensional (2D) materials can take a large amount of mechanical deformation before reaching the fracture limit due to their high Young's modulus, and this in return, provides a way to tune the properties of 2D materials by strain engineering. Previous works have shown that the optical band gap of transition metal chalcogenides (TMDs) can be modulated by strain, resulting in a drift of the photoluminescence (PL) peak position and a decrease (or little change) in PL intensity. Here, we report a member of the post-transition metal chalcogenides (PTMCs), 2D-GaSe sheets, displaying vastly different phenomena under strain. Strained 2D-GaSe emits photons at almost the same wavelength as unstrained material but appears an order of magnitude brighter. In contrast to TMDs, optical spectroscopy measurements reveal that changes in the optical properties are mostly related to the colossal optical absorption anisotropy of GaSe, instead of commonly accepted strain-induced band renormalization. Results suggest that the light–matter interaction and the optical properties of 2D-GaSe can be controlled at will by manipulating the optical absorption.

1 Introduction

GaSe crystals, belonging to the post-transition metal chalcogenides (PTMCs), are a direct gap semiconductor with a band gap of 2.05 eV, and have been widely used in photonics, optoelectronics, and non-linear optics.[1–3] Due to weak van der Waals forces among the layers, the crystal can be easily isolated as few-layer two-dimensional GaSe (2D-GaSe), where each layer is composed of covalently bonded Se–Ga–Ga–Se atoms with D_{3h} symmetry.[2,4,5] Similar to other 2D materials,[6–10] GaSe sheets can also withstand a large amount of strain, thus their properties can be tuned by strain engineering.

Previously, strain-induced changes on the band structure of 2D materials have been demonstrated particularly for group VI-transition metal dichalcogenides (VI-TMDs), such as MoS_2, and group VII-TMDs (such as $ReSe_2$ [11]). Generally, photoluminescence (PL) relies on an energy-level difference between two electron states, which reflects the transition between an excited state and equilibrium state, and is in common use as an important means for probing material properties such as impurity, light-emitting mechanism, impurity defect energy level, and so on. Under external stimuli (strain), the band structure of VI-TMDs changes from direct to indirect and the optical band gap value decreases, resulting in much weaker photon emission and a red-shift in the PL peak position.[6] Even though VII-TMDs also belong to the TMD family, the extra electron in the outmost orbital of the transition metal atom changes the fundamental behavior of strain-induced changes in their properties. For instance, emission from strained VII-TMDs is red-shifted, similar to MoS_2, but the PL intensity remains almost the same due to the lack of an indirect to direct gap transition.[11] Although current strained 2D-materials can provide some new phenomena, the reduction in light emission and red-drift in the PL peak position limit their applications. Therefore, 2D GaSe, which belongs to another class of material, PTMCs, and emits photons at the same wavelength without any significant changes under strain and with stronger emission than the unstrained material, will be more suited for flexible optoelectronic applications than TMDs.

This work addresses this need by experimental and theoretical studies on the strain-induced changes in the optical-electronic features of few-layer GaSe. Strained few-layer GaSe samples were fabricated by depositing the few-layer GaSe onto

[a]The MOE Key Laboratory of Weak-Light Nonlinear Photonics, Taida School of Physics, Nankai University, Tianjin 300457, China
[b]CAS Key Laboratory of Nanosystem and Hierarchical Fabrication, National Center for Nanoscience and Technology, Beijing 100190, China. E-mail: liuq@nanoctr.cn
[c]School of Materials Science and Engineering, Beihang University, Beijing 100191, China
[d]School for Engineering of Matter, Transport and Energy, Arizona State University, Tempe, AZ 85287, USA. E-mail: sefaattin.tongay@asu.edu
[e]Department of Materials Science and Engineering, Massachusetts Institute of Technology, Cambridge, Massachusetts 02139, USA. E-mail: ataca@mit.edu
[f]State Key Laboratory of Superlattices and Microstructures, Institute of Semiconductors, Chinese Academy of Science, Beijing 100083, China. E-mail: jbli@semi.ac.cn

†Electronic supplementary information (ESI) available: Sample preparation and methods, atomic force microscopy measurements, EDX of GaSe nanosheet and density functional theory calculations. See DOI: 10.1039/c5nr08692b

‡These authors contributed equally.

flexible pre-strained Gel-film substrates and then releasing the Gel-film strain to create wrinkled (strained) features. In stark contrast to TMDs, strained regions display an order of magnitude larger PL emission intensity that appears to be at almost the same wavelength as un-strained parts. Based on our micro-absorption and UV-VIS measurements, as well as theoretical calculations, we attribute these effects to much increased photon absorption on wrinkled (strained) regions with an optically absorbent component perpendicular to the incoming light source due to the large optical absorption anisotropy ($\alpha_{\perp} \gg \alpha_{\parallel}$) observed in GaSe. The overall result presents the first experimental demonstration of strain-induced changes in PTMCs, and also suggests unique routes to manipulate the optical properties of layered materials with large optical absorption coefficient anisotropy.

2 Results and discussion

The GaSe crystal with a hexagonal structure is a member of the layered PTMCs. In each layer (Se–Ga–Ga–Se), Ga atoms are sandwiched between Se atoms adding up to ~7.98 Å thickness per sheet and these layers are held together by weak van der Waals forces (Fig. 1a).[1,12] Few-layer 2D GaSe was mechanically exfoliated using Scotch-tape from bulk GaSe crystals grown by a modified Bridgman technique and the structure was analyzed by using transmission electron microscopy (TEM) (Fig. 1b–d). From the high-resolution TEM (HRTEM) pattern (Fig. 1b), it can be observed that distinct and periodic atomic arrangements are obtained for the few-layer GaSe, revealing a high quality crystal characteristic. The corresponding Fast Fourier Transform (FFT) image (Fig. 1c) and the selected area electron diffraction (SAED) image (Fig. 1d) both show one set of clear and distinct six-fold symmetry diffraction spots, further supporting its high crystallinity and hexagonal symmetry. Prominent (002) XRD reflection peaks, associated with lattice reflections from layers in hexagonal (2H-) phase, were observed on all the synthesized materials, and the average single crystalline domain size was estimated at ~50 nm based on Scherrer's formula using the (004) peak FWHM value and Cu Kα wavelength radiation (ESI Fig. S1†). The chemical compositions of the nanosheets were measured by energy dispersive X-ray spectroscopy (EDX), yielding a Ga/Se stoichiometric ratio of ~1 : 1 (standard deviation ~0.05% see ESI Fig. S1†).

To prepare the strained samples, the few-layer GaSe was first mechanically exfoliated from in-house grown GaSe crystals onto a 300 nm thermal oxide on Si substrate (SiO_2/Si). A 200–300 nm thick PMMA film was spin-coated onto the GaSe/SiO_2/Si by a spin coater at 4000 rpm for 1 minute and was then baked at 180 °C for 10 minutes on a heating plate to increase adhesion between PMMA and GaSe flakes. After this, the PMMA/GaSe film was decoupled from SiO_2/Si after etching the sacrificial SiO2 layer by immersing the PMMA/GaSe/SiO_2/Si into 5 mol L^{-1} aqueous NaOH solution at 60 °C for 2 hours. This was followed by cleaning in deionized water. The PMMA/GaSe film was then transferred onto the pre-strained elastomeric Gel-film (a PDMS polymeric film), along the stretching direction with a defined tensile pre-strain of $\varepsilon = \Delta L/L$, where L represents the original length of the Gel-film and ΔL is the elongation after pre-stretching (the schematic diagram of the experimental procedure is showed in ESI Fig. S2 and S3†). Experiments found that well-defined wrinkles on GaSe sheets accounted for releasing the 20% pre-strain, as shown in Fig. 2a and b. AFM images of wrinkled few-layer GaSe with a thickness of 5 nm (about six layers, ESI Fig. S4†) display a lateral periodicity of ~1.4 μm and an average height of 70 nm, as shown in Fig. 2c. This observation agrees well with the phase pattern

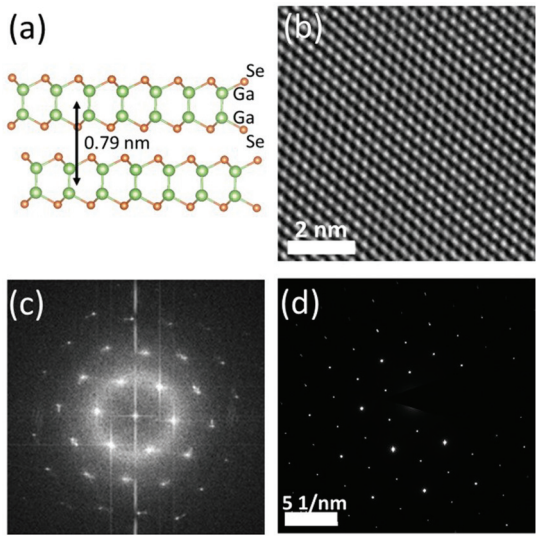

Fig. 1 Few-layer GaSe crystal structure and its TEM images. (a) Layered crystal structure of GaSe with each tetra-layer (TL) formed by Se–Ga–Ga–Se atomic sheets. (b) High resolution TEM images from few-layer GaSe. Fast Fourier Transform (c) and SAED pattern (d).

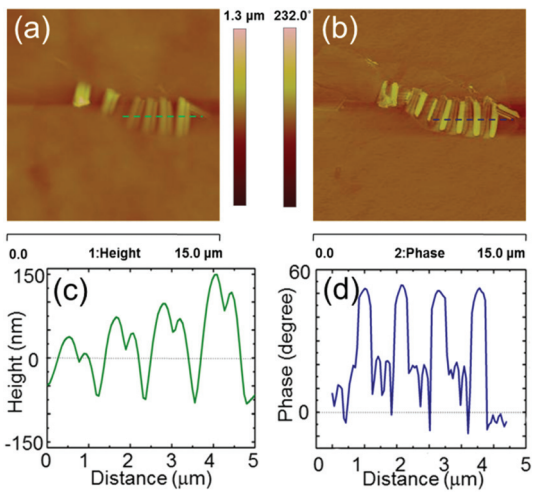

Fig. 2 Atomic force microscopy measurements of wrinkled GaSe sheets. (a) AFM topography and (b) AFM phase mode images of few-layer wrinkled GaSe. (c and d) The corresponding height and phase profiles of sheets shown in (a and b).

from AFM measurements shown in Fig. 2d, which displays a 40° active phase shift.

The periodicity of the strain-induced wrinkles can be described by:[13–16]

$$\lambda_0 = 2\pi h\left[\frac{E}{12\Lambda\mu_S(1-\nu^2)}\right]^{1/3}. \quad (1)$$

In eqn (1), ν and E represent the Possion's ratio and Young's modulus of GaSe, respectively. Here we take ν = 0.186, E = 34 GPa and $\Lambda = ((1+\varepsilon_{pre})^3 + 1)/2(1+\varepsilon_{pre})$, where ε_{pre} refers to the pre-strain amount of the Gel-film.[17] As $\mu_s \approx 20$ kPa is the shear modulus of the flexible substrate, the value of λ_0, calculated using eqn (1), is found to be ~317h, where $h \sim 5$ nm is the thickness of GaSe. Using this value, the corresponding wavelength of the strained six-layer GaSe is ~1.5 μm, which is in close agreement with our experimental value (~1.4 microns). Here, we note that these self-formed wrinkles are always perpendicular to the direction of applied stress due to a mismatch between elastic modulus values of GaSe and the Gel-film. By applying different pre-strains (from 20% to 100%) and a gradually releasing process, some representative types of morphologies of the strained few-layer GaSe are exhibited in Fig. S3.† With increase of the pre-strain, scanning electron microscopy (SEM) images show the evolution from rippled wrinkles (Fig. S3a†) to standing folds (Fig. S3b and c†), eventually to collapsed folds (Fig. S3d†). Since the well-shaped rippled wrinkles are unsustainable when the pre-strain added exceeds a certain degree (>30%), and considering a PL microprobe with one micrometer scale, we choose the sample at a pre-strain of 20% (Fig. 2a) for our investigation. For the sample, flat (unstrained) and wrinkled (strained) regions are formed, and the maximum uniaxial local strain ε on the top of wrinkled regions can be expressed as:[18,19]

$$\varepsilon \sim \pi^2 h\delta/\lambda^2(1-\nu^2), \quad (2)$$

where λ and δ denote the width and height of wrinkles of the strained few layer GaSe, which can be characterized by AFM, as shown in Fig. 2. According to eqn (2), local uniaxial strain on the top of wrinkled 2D-GaSe reaches up to 0.3%. In the remainder of this article, 'strained' and 'wrinkled' will be used interchangeably to refer to strained GaSe.

To understand the effects of strain on the optical properties of 2D-GaSe, the PL spectra of strained and flat GaSe regions were measured (Fig. 3) for few-layer GaSe with different thickness, different profiles and even different substrates. Interestingly, the single scan PL spectrum of a strained region (Fig. 3a) shows that the PL intensity is about 10 fold greater than that of an unstrained region, and their emission peaks appear at the same position. These results were reproduced on more than twenty (20) separate sets of samples with PL enhancement factors ranging from half to one and a half orders of magnitude. Similar measurements were also reproduced on another kind of typically strained GaSe sheet (Fig. 3b and c) formed by the exfoliation process on SiO_2/Si. Pink regions correspond to the strained (wrinkled) GaSe (region #1) and lie

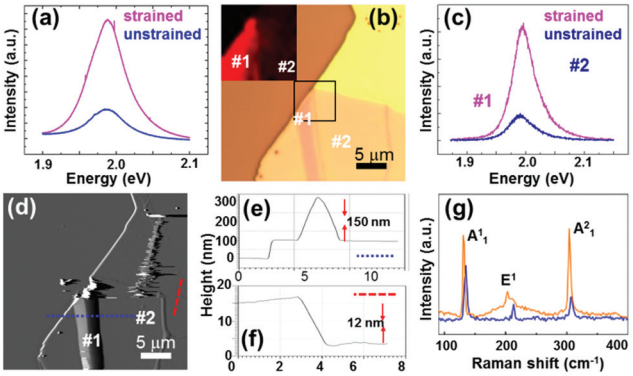

Fig. 3 Photoluminescence enhancement and lattice vibration of 2D-GaSe by strain engineering. (a) PL spectra taken from wrinkled and unwrinkled regions in Fig. S4.† (b) Optical image of a wrinkled GaSe flake formed during the exfoliation process. Region #1 is strained and region #2 is flat. Inset: PL mapping of the highlighted region. (c) PL spectra obtained from region #1 and region #2. (d) AFM image of the same flake shown in (b). (e and f) AFM line scan data taken across the wrinkled (blue dotted line) and red dashed regions. The latter measurement was performed to estimate the thickness of the overlying flake. (g) Raman spectra observed for regions without wrinkles (blue) and with wrinkles (orange) on the same GaSe nanosheets shown in Fig. S4.†

over the unstrained (unwrinkled) GaSe sheets (region #2). The AFM image in Fig. 3d shows that the wrinkled region #1 lies over the flat region (region #2), and is 150 nm in height (Fig. 3e) and 12 nm in thickness (about 15 layers, Fig. 3f). Importantly, our PL mapping measurements (Fig. 3b inset) still show that region #1 (strained region) is nearly an order of magnitude more luminescent compared to flat regions, indicating that the PL enhancement is independent of substrate type. Since the 12 nm-thick piece is on top of a 100 nm flake which also contributes to the PL signal, it is hard to evaluate only the thickness effect on the PL enhancement by this experiment. However, the effect of thickness cannot be ruled out based on eqn (2) and warrants further study. Consistent with the PL mapping, the single scan PL spectrum of region #1 (Fig. 3c) shows that the PL intensity is greater than that of region #2 without peak position drift, further confirming the PL enhancement without peak-shifted emission for different profiles and even different substrates. TMDs have strain-dependent PL emission wavelengths and under strain have much weaker photoluminescence (due to the strain induced direct to indirect band gap transition). In this regard, 2D-GaSe sheets are at least an order of magnitude more luminescent and the light emission remains at the same wavelength displaying stark differences compared to the previous studies on TMDs.

Considering that the total amount of material on a wrinkled region is slightly (~10%) more than on unwrinkled parts due to geometrical considerations, this difference can only contribute to less than 10% of the PL enhancement, and thus an additional mechanism is necessary to explain the phenomenon. Before discussion of the mechanism, we have to exclude another possible effect from morphology deformation. As we

well know, Raman spectroscopy has been widely used for verifying the effect of strain on 2D materials, such as graphene and MoS_2,[13,20–22] by the shifts and shapes of peaks corresponding to the phonon modes of the 2D materials, therefore Raman spectroscopy will provide strain-induced information. Our Raman spectroscopy measurements on wrinkled few-layer 2D-GaSe display three prominent peaks located at 136 cm^{-1}, ~200 cm^{-1}, and 310 cm^{-1} corresponding to A^1_{1g}, E^1_{2g}, and A^2_{1g} modes (Fig. 3g and Fig. S5a†). Obviously, A^1_{1g} and E^1_{2g} modes have a slight drift to lower frequencies with respect to the unstrained region, similar to the observations on MoS_2,[18] and this is consistent with calculated frequency shifts under 0.3% strain that can be up to 5 cm^{-1}, as shown in Fig. S5b.† Here, we note that the in-plane E_{2g} mode of GaSe shifts by greater amount compared to the out-of-plane A_{1g} mode. We attribute this to the applied lateral strain greatly acting on each individual layer instead of greatly changing the interlayer coupling strength (which couples to the A_{1g} mode). Softening of Raman modes around 200 cm^{-1} for in-plane modes in the wrinkles is not only from softening of the E^1 mode, but also from the activation of Raman active E^2 modes (no. 13–16 in Fig. S6†). These results suggest that strain affects vibration of Se atoms more than Ga atoms during strain. From the analyses above, the strain has obviously occurred on top of wrinkled few-layer GaSe flakes and produced an effect on the vibrational modes, further confirming that the PL enhancement comes from strain rather than surface geometry deformation.

Since PL enhancement is not generated by 10% area increment and surface geometry deformation, an internal mechanism induced by strain should be discussed. Generally, strain can lead to a transition in the band-gap of 2D semiconductors, but in our case of PL, peak position drift is negligible (~20 meV) under strain despite the dramatic increase in integrated PL intensity, which implies that the observed effects are not due to the strain induced band renormalization like group VI TMDs. In Fig. 4a and b, we present our theoretical simulation results to understand how the electronic structure of few-layer (1 and 3) and bulk GaSe are affected *via* Density Functional Theory (DFT) calculations. The Γ-point in the valance band edge is dominated by p_z orbitals of chalcogen atoms and metal. Any lateral strain will not have any effect on charge distribution. The Γ-point in the conduction band is a combination of p_x and p_y orbitals of only chalcogen atoms. As the number of layers in the simulation cell increases, the effect of lateral strain on the direct gap at the Γ-point decreases from ~150 meV in a monolayer to ~30 meV in the bulk limit under 0.3% applied strain. Since band renormalization results in changes much greater than 20 meV, we eliminate the possibility of strain induced changes in the optical band gap.

Another optical effect is related to the optical absorption coefficient of the overlying material (GaSe or GaS). This is particularly important for layered PTMCs, such as GaS, GaSe and GaTe, where the optical absorption coefficient can be more than an order of magnitude different depending on the polarization conditions.[23] For example, when the absorption coefficient of GaSe crystals probed in normal incident light is

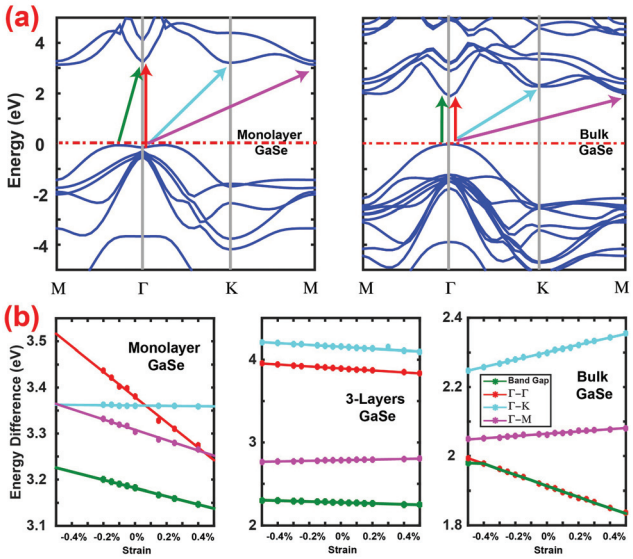

Fig. 4 Band structure of GaSe under strain. (a) Electronic band structure of monolayer and bulk-GaSe calculated using DFT. Fermi energy is indicated by the red dashed lines. Arrows indicate special high symmetry transitions from valance to conduction band. Green, red, cyan and magenta arrows are from VBM (valance band maximum) to Γ-point, Γ-point to Γ-point, Γ-point to *K*-point, and Γ-point to *M* point, respectively. (b) Change in the energy difference of high symmetry points under strain (±0.5%) of few-layer and bulk GaSe.

polarized perpendicular ($\alpha_\perp$, flat region) and parallel ($\alpha_\parallel$, strained configuration) to the *c*-axis, the absorption coefficient ratio ($\alpha_\perp/\alpha_\parallel$) reaches up to 40.[23] This implies that once the wrinkles are formed on the few-layer GaSe, the absorption coefficient will be enhanced and the GaSe sheets absorb (and emit) photons more efficiently as the incident light has a finite perpendicular component to the *c*-axis. Our micro-absorption measurements performed on the strained GaSe flake/Gel-film confirm that the absorption is greatly enhanced, as shown in Fig. 5a (red and blue). The main peak at 2 eV corresponds to the band edge absorption, whereas the peak at 3 eV is associated with higher lying electronic bands, which can also be observed in the calculated absorption spectrum in Fig. 5b, similar to the calculated absorption spectrum of monolayer GaSe (where the energy values are off by ~0.2 eV due to DFT functional, but theoretical results behave similarly to experiments). We only calculated absorption spectra for monolayer and bulk structures, but not for a few layers (in this case 5 nm thick 2D-GaSe consists of ~6 layers) due to the extensive computational requirements. The intensity of the 2 eV absorption peak is greatly enhanced for strained regions, implying that the optical absorption coefficient increases rather drastically in agreement with earlier reports on bulk crystals.[23] Consequently, strained regions absorb and emit photons more efficiently (Fig. 3) compared to pristine (unstrained) regions due to an increase in the out-of-plane component of the strained sheets and enhanced optical absorption caused by the large optical absorption anisotropy coefficient. In accordance with the experimental findings, optical absorption

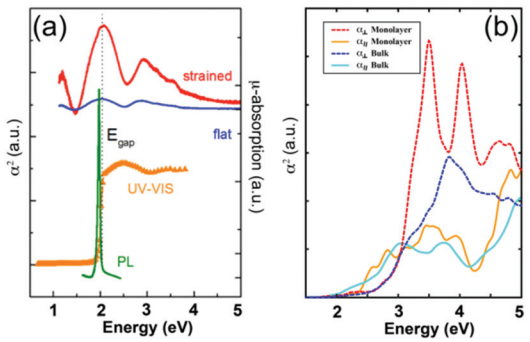

Fig. 5 Enhancement in optical absorption coefficient. (a) Micro-absorption measurements taken from strained (red) and unstrained (blue) regions of 2D-GaSe sheets. Optical absorption from strained regions is greatly enhanced and both regions display a peak at 2 eV corresponding to the fundamental band edge of GaSe as determined by the UV-VIS absorption spectrum taken from bulk GaSe single crystals (orange) and PL emission (green). (b) Calculated absorption spectra of monolayer and bulk GaSe in the perpendicular and parallel directions.

calculations on GaSe thin films performed by density functional theory calculations show that the absorption is enhanced in the perpendicular ($\alpha_\perp$) direction with $\alpha_\perp/\alpha_\parallel \gg 1$. (The highest value calculated up to 5 eV photon energy is ~6 for bulk and ~8 for monolayer structures).

Conclusions

In summary, strain effects on 2D-GaSe, a member of the post-transition metal chalcogenides (PTMCs), were reported for the first time. Strained few-layer GaSe displays an order of magnitude stronger light emission (PL) without any change in its emission peak position (wavelength) for different numbers of a few layers, different profiles, and even different substrates, which is in stark contrast to TMD materials (MoS_2, WS_2, WSe_2, ReS_2 *etc.*) where the PL intensity and the emission wavelength both decrease for an increasing strain value. Optical spectroscopy, micro-absorption, and density functional theory calculations show that the strain-induced PL enhancement in few-layer GaSe is related to the large optical anisotropy observed in GaSe and associated enhancement in the absorption coefficient. This effect is vastly different from strain effects in TMDs where the strain induced changes occur due to strong band renormalization and associated changes in the excitonic dynamics. Overall the results establish the strain-induced effects on GaSe for the first time, providing further insights into strain effects in 2D materials, and enable us to control light–matter interactions at will using optical anisotropy induced by nanoscale strain engineering.

Acknowledgements

This research was supported by the National Natural Science Foundation of China (10974037), the CAS Strategy Pilot program (XAD 09020300), and NBRPC (2010CB934102). J. L. acknowledges financial support from the National Natural Science Foundation of China (2011CB921901). S. T. is supported by Arizona State University, Research Seeding Program.

Notes and references

1 X. Li, M. W. Lin, A. A. Puretzky, J. C. Idrobo, C. Ma, M. Chi, M. Yoon, C. M. Rouleau, I. I Kravchenko, D. B. Geohegan and K. Xiao, *Sci. Rep.*, 2014, **4**, 5497.
2 D. J. Late, B. Liu, J. Luo, A. Yan, H. S. Matte, M. Grayson, C. N. Rao and V. P. Dravid, *Adv. Mater.*, 2012, **24**, 3549–3554.
3 Y. Ma, Y. Dai, M. Guo, L. Yu and B. Huang, *Phys. Chem. Chem. Phys.*, 2013, **15**, 7098–7105.
4 S. Lei, L. Ge, Z. Liu, S. Najmaei, G. Shi, G. You, J. Lou, R. Vajtai and P. M. Ajayan, *Nano Lett.*, 2013, **13**, 2777–2781.
5 X. Meng, A. Pant, H. Cai, J. Kang, H. Sahin, B. Chen, K. Wu, S. Yang, A. Suslu and F. Peeters, *Nanoscale*, 2015, **7**, 17109–17115.
6 H. J. Conley, B. Wang, J. I. Ziegler, R. F. Haglund, Jr., S. T. Pantelides and K. I. Bolotin, *Nano Lett.*, 2013, **13**, 3626–3630.
7 S. B. Desai, G. Seol, J. S. Kang, H. Fang, C. Battaglia, R. Kapadia, J. W. Ager, J. Guo and A. Javey, *Nano Lett.*, 2014, **14**, 4592–4597.
8 C. Lee, X. D. Wei, J. W. Kysar and J. Hone, *Science*, 2008, **321**, 385–388.
9 A. Castellanos-Gomez, M. Poot, G. A. Steele, H. S. J. van der Zant, N. Agrait and G. Rubio-Bollinger, *Adv. Mater.*, 2012, **24**, 772–775.
10 S. Tongay, W. Fan, J. Kang, J. Park, U. Koldemir, J. Suh, D. S. Narang, K. Liu, J. Ji and J. Li, *Nano Lett.*, 2014, **14**, 3185–3190.
11 S. Yang, C. Wang, H. Sahin, H. Chen, Y. Li, S.-S. Li, A. Suslu, F. M. Peeters, Q. Liu and J. Li, *Nano Lett.*, 2015, **15**, 1660–1666.
12 X. Zhou, J. Cheng, Y. Zhou, T. Cao, H. Hong, Z. Liao, S. Wu, H. Peng, K. Liu and D. Yu, *J. Am. Chem. Soc.*, 2015, **137**, 7994–7997.
13 Y. Wang, R. Yang, Z. W. Shi, L. C. Zhang, D. X. Shi, E. Wang and G. Y. Zhang, *ACS Nano*, 2011, **5**, 3645–3650.
14 J. Zang, S. Ryu, N. Pugno, Q. Wang, Q. Tu, M. J. Buehler and X. Zhao, *Nat. Mater.*, 2013, **12**, 321–325.
15 W. Z. Bao, F. Miao, Z. Chen, H. Zhang, W. Y. Jang, C. Dames and C. N. Lau, *Nat. Nanotechnol.*, 2009, **4**, 562–566.
16 Y. P. Cao and J. W. Hutchinson, *J. Appl. Mech.-Trans. ASME*, 2012, **79**, 031019.
17 D. Vella, J. Bico, A. Boudaoud, B. Roman and P. M. Reis, *Proc. Natl. Acad. Sci. U. S. A.*, 2009, **106**, 10901–10906.
18 A. Castellanos-Gomez, R. Roldan, E. Cappelluti, M. Buscema, F. Guinea, H. S. van der Zant and G. A. Steele, *Nano Lett.*, 2013, **13**, 5361–5366.

19 S. Yang, C. Wang, H. Sahin, H. Chen, Y. Li, S.-S. Li, A. Suslu, F. M. Peeters, Q. Liu, J. Li and S. Tongay, *Nano Lett.*, 2015, **15**, 1660–1666.
20 C. R. Zhu, G. Wang, B. L. Liu, X. Marie, X. F. Qiao, X. Zhang, X. X. Wu, H. Fan, P. H. Tan, T. Amand and B. Urbaszek, *Phys. Rev. B: Condens. Matter*, 2013, **88**, 121301.
21 K. Zhang, S. Hu, Y. Zhang, T. Zhang, X. Zhou, Y. Sun, T.-X. Li, H. J. Fan, G. Shen and X. Chen, *ACS Nano*, 2015, **9**, 2704–2710.
22 Z. H. Ni, T. Yu, Y. H. Lu, Y. Y. Wang, Y. P. Feng and Z. X. Shen, *ACS Nano*, 2008, **2**, 2301–2305.
23 R. Le Toullec, N. Piccioli, M. Mejatty and M. Balkanski, *Il Nuovo Cimento B Series 11*, 1977, **38**, 159–167.